APPLIED AND ENVIRONMENTAL MICROBIOLOGY, Aug. 2005, p. 4809–4821 Vol. 71, No. 8
0099-2240/05/$08.00+0 doi:10.1128/AEM.71.8.4809–4821.2005

Characterization of Colony Morphology Variants Isolated from *Pseudomonas aeruginosa* Biofilms

Mary Jo Kirisits,[1,2] Lynne Prost,[2]† Melissa Starkey,[3] and Matthew R. Parsek[2,3]*

Department of Civil, Architectural, and Environmental Engineering, The University of Texas at Austin, Austin, Texas 78712[1]; Department of Civil and Environmental Engineering, Northwestern University, Evanston, Illinois 60208[2]; and Department of Microbiology, The University of Iowa, Iowa City, Iowa 52242[3]

Received 6 December 2004/Accepted 7 March 2005

In this study, we report the isolation of small, rough, strongly cohesive colony morphology variants from aging *Pseudomonas aeruginosa* PAO1 biofilms. Similar to many of the *P. aeruginosa* colony morphology variants previously described in the literature, these variants autoaggregate in liquid culture and hyperadhere to solid surfaces. They also exhibit increased hydrophobicity and reduced motility compared to the wild-type parent strain. Despite the similarities in appearance of our colony morphology variant isolates on solid medium, the isolates showed a range of responses in various phenotypic assays. These variants form biofilms with significant three-dimensional structure and more biomass than the wild-type parent. To further explore the nature of the variants, their transcriptional profiles were evaluated. The variants generally showed increased expression of the *psl* and *pel* loci, which have been previously implicated in the adherence of *P. aeruginosa* to solid surfaces. When a mutation in the *psl* locus was introduced into a colony morphology variant, the colony morphology was only partially affected, but hyperadherence and autoaggregation were lost. Finally, similar colony morphology variants were found in isolates from cystic fibrosis patients. These variants displayed many of the same characteristics as the laboratory variants, suggesting a link between laboratory and cystic fibrosis biofilms.

Many bacteria in clinical and natural environments are members of biofilm communities, which are assemblages of microorganisms attached to a solid surface and encased in an extracellular polymeric matrix. Advantages to being in a biofilm community include facilitation of metabolic interactions due to the cells' close physical proximity, increased horizontal gene transfer, and protection from predation and antimicrobial stress. However, the biofilm lifestyle undoubtedly has disadvantages as well. For example, high cell densities can result in severe, dynamic gradients of nutrients and toxic metabolic by-products. Bacteria may cope with these stressors in a variety of ways. First, motile bacteria may leave the biofilm. This appears to be an active process for some bacteria, and recent reports suggest that starvation may trigger cell detachment from a biofilm (17, 29). However, leaving the biofilm causes the bacteria to lose biofilm-derived advantages. Second, a cell's physiology may be fine-tuned for a particular biofilm niche. The "biofilm phenotype," or the expression of specific genes and proteins associated with the biofilm lifestyle, has been the focus of recent research (36, 39). Third, mutation is a powerful means by which bacteria can adapt to stressful environments (3, 23).

Pseudomonas aeruginosa is a model organism for the study of biofilm communities, and research in the last decade has uncovered many of the molecular determinants that contribute to biofilm formation by this organism. Recent reports indicate that different types of environmental pressures select for colony morphology variants of *P. aeruginosa*, and many of these variants also have biofilm-related phenotypes. The literature describes the appearance of these variants on solid growth medium by several names: small-colony variants (SCVs), rough small-colony variants (RSCVs), wrinkled variants, autoaggregating cells, and rugose colonies. Drenkard and Ausubel (9) reported that treatment of *P. aeruginosa* PA14 with the antibiotic kanamycin resulted in the appearance of kanamycin-resistant RSCVs on solid growth medium. RSCVs displayed hyperadherence, and the frequency of occurrence of this variant appeared to be negatively controlled by the two-component system response regulator homolog PvrR. They hypothesized that biofilm growth and antibiotic treatment selected for these variants and that this phenotype may play a role in the chronic colonization of the cystic fibrosis (CF) lung. Déziel et al. (8) isolated a number of colony morphology variants from *P. aeruginosa* 57RP standing liquid cultures and biofilms growing on hexadecane. These variants were generally characterized by hyperadherence, hyperpiliation, reduced motility, increased hydrophobicity, and increased susceptibility to hydrogen peroxide. From a drip reactor inoculated with *P. aeruginosa* PAO1, Boles et al. (4) isolated colony morphology variants that were hyper-biofilm formers and had an increased resistance to hydrogen peroxide compared to the wild-type parent strain.

Colony morphology variants have also been isolated from clinical environments. Häußler et al. (14) described *P. aeruginosa* SCVs that were derived from CF patients; these variants

* Corresponding author. Mailing address: University of Iowa, Department of Microbiology, 540E EMRB, Iowa City, IA 52242. Phone: (319) 335-8228. Fax: (319) 335-7949. E-mail: matthew-parsek@uiowa.edu.

† Present address: Department of Microbiology, University of Washington, Seattle, WA 98195.

TABLE 1. Strains and plasmids used in this study

Strain (colony morphology) or plasmid	Relevant characteristic(s)	Source or reference
P. aeruginosa strains		
PAO1 (WT)	Wild-type *P. aeruginosa* strain PAO1	
PAO1 *lasB*::*gfp* (WT)	Harbors a mini-Tn*5* insertion containing a transcriptional fusion between *lasB* promoter and gene encoding the green fluorescent protein (*gfp*)	This study
MJK8, MJK123 (ST)	ST isolates from tube biofilm experiments with PAO1	This study
MJK3, MJK22–30 (ST)	ST isolates from tube biofilm experiments with PAO1 *lasB*::*gfp*	This study
PAO1-Tn*7*-*gfp* (WT)	Tn*7* chromosomal insertion of *gfp*	This study
PAO1-*psl* (WT)	*psl* deletion mutant (PA2232–PA2235)	This study
MJK8-*psl* (ST)	*psl* deletion mutant (PA2232–PA2235)	This study
009 37s (ST)	Clinical isolate from CF lung	5
009 38s (ST)	Clinical isolate from CF lung	5
009 39s (ST)	Clinical isolate from CF lung	5
CF127 (ST)	Clinical isolate from CF lung	40
Plasmids		
pMRP9	Plasmid with *gfp* under control of Tac promoter, carbenicillin resistance (Cb^r)	7
pEX18.Ap	Suicide plasmid used for construction of allelic replacements in *P. aeruginosa*, ampicillin resistance (Ap^r)	16
pMO011305	Cosmid harboring the PA2231–PA2241 genes of the *psl* locus, tetracycline resistance (Tc^r)	18
pMPSL-KO1	Suicide plasmid containing gentamicin (Gm) cassette insertion in *psl* locus, Gm^r and Ap^r	This study

exhibited hyperadherence and increased type IV pili-mediated twitching motility. While the laboratory-derived, spontaneous variants may have a single mutation relative to the parent strain, the clinical variants probably accumulate multiple mutations in the CF lung. Different mutations may contribute to the range of phenotypes observed in the clinical isolates. As expected, some laboratory-derived colony morphology variants have been shown to result from single mutations. D'Argenio et al. (6) demonstrated that a mutation in *wspF* (PA3703) resulted in the formation of an autoaggregative SCV exhibiting defects in swimming, twitching, and swarming motilities. *wspF* is located within a locus on the PAO1 chromosome (PA3702 to PA3708) that displays homology to chemosensory proteins. A regulator controlling this phenotype, WspR, possesses a GGDEF domain that has been implicated in the synthesis of the intracellular signaling molecule, cyclic di-GMP. Taken together, the studies in the literature suggest two things. First, autoaggregating cells form colonies with a distinctive morphology and are associated with enhanced biofilm formation and chronic CF infection, and second, although colony morphology variants from different studies may appear similar on solid medium and in liquid culture, they can differ significantly for other phenotypes.

In this study, we isolated and characterized colony morphology variants from laboratory-grown biofilms of *P. aeruginosa* PAO1. One class of these variants, which we call "sticky" (ST), are similar to the colony morphology variants described in the literature: autoaggregating in liquid culture and displaying a hyper-biofilm-forming phenotype. Despite the aforementioned similarities among our colony morphology variants, different isolates showed a range of responses in phenotypic assays. Transcriptional profiling was performed on ST variants, and it indicated that type IV pili and two putative exopolysaccharide (EPS) loci were up-regulated. Mutational analysis of one of the EPS loci, the *psl* locus (PA2231 to PA2245), indicated that this locus contributes significantly to the autoaggregation and hyperadherence of the ST variant but only partially to the colony morphology on solid growth medium. Analysis of clinical isolates displaying the ST colony morphology showed that these isolates share many of the phenotypic traits of the laboratory-derived biofilm ST isolates.

MATERIALS AND METHODS

Bacterial strains, strain construction, and growth media. Table 1 shows the *Pseudomonas aeruginosa* strains used in this study. The laboratory-derived phenotypic variants were generated, as described below, in independent tube biofilms, and the clinically derived phenotypic variants were obtained from CF patients. The phenotypic variants have small, rough, highly cohesive colonies and are described as having the sticky or ST colony morphology. The phenotypic variants look red when grown on Congo red agar (Luria-Bertani [LB], 1.6% agar, 2% [vol/vol] Congo red solution [2 mg/ml Congo red, 1 mg/ml Coomassie brilliant blue, 70% {vol/vol} ethanol]) (26). In Table 1, each strain is described according to its colony morphology: wild-type (WT) or ST. Unless otherwise noted, strains were grown at 37°C in LB medium. Where noted, the strains were grown in baffled flasks containing a stir bar to minimize aggregation in the phenotypic variants. For plasmid selection, 300 μg/ml carbenicillin, 100 μg/ml gentamicin, or 50 μg/ml tetracycline was used with *P. aeruginosa*, and 15 μg/ml gentamicin, 100 μg/ml ampicillin, or 5 μg/ml tetracycline was used with *Escherichia coli*.

Strains PAO1 *lasB*::*gfp* and PAO1-Tn*7*-*gfp* were constructed through transposon insertion into the chromosome as previously described (20). Construction of *psl* allelic replacements was conducted as follows. A region of genomic DNA containing genes PA2232 to PA2235 of the *psl* locus was amplified using primers MPSL-UP (5′-GCGGTACCGCTGTTCCGCACCCTGGACGACT-3′) and MPSL-DN (5′-CGCAAGCTTCCTTGCCGAACGCCGTGGTGA-3′). The PCR product was ligated to the suicide vector pEX18.Ap via KpnI and HindIII restriction sites. PA2233 to PA2234 and parts of PA2232 and PA2235 were replaced by a blunt-ended SacI fragment containing the gentamicin resistance cassette from pPS858 (16). The resulting plasmid, pMPSL-KO1, was mated into PAO1 and MJK8, and mutants were selected on *Pseudomonas* isolation agar containing 200 μg/ml gentamicin. Double recombinant mutants were selected on LB plates containing 5% sucrose. Double recombinant mutants PAO1-*psl* and MJK8-*psl* were confirmed by PCR.

To determine which environmental pressures might select for ST variants, planktonic WT cells were exposed to a variety of culture conditions. Several culture conditions were tested: pH variation (7, 8, 9, and 10), hydrogen peroxide stress (0.003, 0.006, and 0.012%), osmotic stress (0.5, 1.0, and 1.5% sodium chloride), anaerobic conditions, exposure to spent LB medium (from a stationary-phase culture of PAO1), and growth in various media (i.e., defined media:

Jensen's medium [19], which contains 1.26% glucose, modified Jensen's medium [0.126% glucose], M9 medium with no carbon source [2], M9 medium supplemented with 0.033% $MgSO_4$ and 1.26% glucose, and EPRI medium [7], which contains 0.005% sodium lactate and 0.005% sodium succinate). The cultures were incubated at room temperature (~22°C) with shaking for 15 days, followed by a period of stagnation for 12 days. Samples were periodically removed, serially diluted, spot plated (10 μl spots) onto LB agar plates, and incubated overnight at 37°C. WT and ST colonies were enumerated on the following day.

T-RFLP. Terminal restriction fragment length polymorphism (T-RFLP) was performed on WT (PAO1) and ST (MJK8). Primers 8f (5′-AGAGTTTGATC CTGGCTCAG-3′) (1) and 926r (5′-CCGTCAATTCCTTTRAGTTT-3′) (22) were used to amplify a fragment of the 16S rDNA; the forward primer was fluorescently labeled at the 5′ end (IRDye 800; LI-COR Biosciences, Lincoln, NE). Each 50-μl PCR mixture contained 1.25 U *Taq* DNA polymerase, 10 mM Tris-HCl, 50 mM KCl, 1.5 mM $MgCl_2$, 0.2 mM concentrations of each deoxynucleoside triphosphate, 0.2 μM concentrations of each primer, and 1 μl of an overnight culture and was amplified according to the method of Urakawa et al. (35). The amplicon was purified (QIAquick kit; QIAGEN, Inc., Valencia, CA), and 100 ng of purified amplicon was digested with 40 U HhaI in a 20-μl reaction mixture at 37°C for 6 h. Two microliters of each digest was mixed with 2 μl of stop solution (LI-COR Biosciences, Lincoln, NE). The samples and size markers (50 to 700 base pairs; LI-COR Biosciences, Lincoln, NE) were denatured at 95°C for 2 min and chilled for 10 min on ice. They were loaded onto a 5.5% polyacrylamide gel, and the fluorescently labeled fragments were separated on a DNA sequencer (model 4000L; LI-COR Biosciences, Lincoln, NE). BaseImagIR software (version 2.31; LI-COR Biosciences, Lincoln, NE) was used for data collection. The size of each band in the T-RFLP pattern was calculated using Gene Profiler 4.03 (Scanalytics, Inc., Fairfax, VA).

Growth curve experiments. To determine doubling times, the appropriate strains were inoculated to separate 250-ml baffled Erlenmeyer flasks containing 50 ml LB and a stir bar. The flasks were incubated at 37°C with shaking, and samples were removed periodically over a 3-h period. Each sample was divided into aliquots to measure growth in two different ways: optical density at 600 nm (OD_{600}) and protein. The OD_{600} sample aliquots were vortexed for 10 s, and OD_{600} was measured in duplicate. The cells from the protein sample aliquot were pelleted, washed, and resuspended in 100 mM Tris-HCl (pH 7.2). Three aliquots of the resuspended cells were placed in a microtiter plate, and the cells were lysed in a microplate horn sonicator (20 kHz, XL-2020; Misonix, Inc., Farmingdale, NY). The cells were sonicated for 1 min at an output of 7.5, followed by a rest period of 1 min; this cycle was repeated a total of 12 times. The lysed cells were subjected to a standard microplate protein assay (Coomassie Plus protein assay reagent kit; Pierce Biotechnology, Inc., Rockford, IL).

Microtiter plate adhesion assay. Biofilm formation was examined by the method of O'Toole and Kolter (24) with a few modifications. One microliter of a late-log-phase culture was added to 99 μl LB in a 96-well microtiter plate, incubated for 10 h at 37°C, and rinsed thoroughly with water to remove nonadherent cells. Crystal violet (125 μl, 1% [wt/vol]) was added to each well, incubated for 15 min, and rinsed thoroughly with water. To solubilize the crystal violet, 200 μl of 95% ethanol was added to each well and mixed. A 100-μl aliquot was removed to a new well, and the absorbance was read at 595 nm. At least three replicates were done for each strain.

Motility assays. Swimming and twitching motilities were assessed as described previously (8) but with the following modifications. Swim plates were stab inoculated with sterile 10-μl pipette tips and incubated for 20 h at 30°C; twitch plates were stab inoculated with 10-μl pipette tips and incubated at 30°C for 44 h. Four replicates were run for each assay.

Microbial adhesion to hydrocarbon (MATH) test. To compare the relative hydrophobicities of various *P. aeruginosa* strains, cell adherence to hexadecane was determined as described previously (8).

Liquid culture quorum-sensing induction experiments. Quorum-sensing induction was compared between reporter strains PAO1 *lasB*::*gfp* and MJK3 (*lasB*::*gfp*). The strains were grown from freezer stock and subcultured twice at low optical densities to ensure that quorum sensing was not induced in the inoculum. One hundred microliters of the inoculum (OD_{600} = 0.1) was added to 20 ml LB in a 250-ml baffled Erlenmeyer flask with a stir bar and incubated at 37°C with shaking. Samples were taken at regular intervals. The cells were pelleted and resuspended in 1× phosphate-buffered saline (PBS). The OD_{600} and fluorescence were measured for each sample. Fluorescence measurements were made using an FL_X800 microplate fluorescence reader (Bio-Tek Instruments, Inc., Winooski, Vermont) with an excitation wavelength of 485 ± 20 nm, an emission wavelength of 530 ± 25 nm, and a sensitivity of 120.

EPS analysis. PAO1 and MJK8 were grown on cellophane sheets on LB plates, and soluble EPS was isolated as described previously (42). Samples were sent to the University of Georgia's Complex Carbohydrate Research Center for glycosyl composition analysis. The EPS composition was reported as the mole percent of total carbohydrate.

Antibiotic susceptibility assays. A rotating-disk biofilm reactor (15) was used to test the resistance of biofilm and planktonic cells to antimicrobial compounds. The resistances of PAO1 and MJK8 to tobramycin and chlorine were tested. The chemostat contained 250 ml LB, which was inoculated with the appropriate strain and stirred in batch mode overnight at room temperature. The following day, the reactor was operated as a chemostat with a dilution rate of 0.1 h^{-1} for 24 h. Then the stir bar was replaced with a disk containing 18 removable polycarbonate chips, and biofilm formation proceeded for 24 h. At this time, the disk and an aliquot of planktonic cells were removed from the reactor. The polycarbonate chips were rinsed in 1× PBS to remove loosely attached cells, and the intact biofilms were used for antimicrobial testing. Equal numbers of biofilm and planktonic cells, as determined by viable plate counts, were exposed to tobramycin (0 to 100 μg/ml) and chlorine (0 to 100 mg/liter) in 1× PBS for 5 h at 37°C. The biofilm chips or planktonic cells were then removed to fresh 1× PBS, sonicated for 10 min (38.5 to 40.5 kHz), and briefly vortexed. Microscopy was performed to verify that sonication separated ST cultures into single cells. Plate counts were performed as described above. Analysis of colony morphologies on solid medium verified that conversion of WT to ST and reversion of ST to WT did not occur during the experiment.

Flow cell biofilm reactors. *P. aeruginosa* biofilms were grown at room temperature with Jensen's medium in polycarbonate flow cells with channel dimensions of 1 by 4 by 40 mm in a procedure similar to that previously described (15).

For monoculture biofilms (e.g., PAO1/pMRP9 or MJK8/pMRP9), biofilm structure was examined after 3 days by confocal laser-scanning microscopy (CLSM) (Zeiss LSM 510; Carl Zeiss, Inc., Jena, Germany). For coculture biofilms, (e.g., 50% PAO1-Tn*7*-*gfp*–50% MJK8 inoculum), biofilms were sacrificed on days 3, 4, and 8. For visualization of the untagged cells (MJK8), the biofilms were stained with a 1:20 dilution of Syto 62 (Molecular Probes, Inc., Eugene, OR) in Jensen's medium.

Tube biofilm reactors. The tube biofilm system was configured as described previously (30) except that 2.4-mm-inner-diameter silicone tubing was used to house the biofilm.

Tube biofilms were grown with one of several inocula: PAO1, PAO1 *lasB*::*gfp*, or MJK3. The biofilms were sacrificed at various times during the experiment for cell harvesting. To harvest cells, the biofilm tubing was removed from the flow path, cut into several smaller pieces, and placed in a Microfuge tube with sterile 1× PBS. This tube was sonicated for 1 min, chilled on ice for 1 min, and vortexed for 1 min; this cycle was repeated four times. The tubing was removed to a fresh Microfuge tube, and any cells remaining in the tubing were pelleted in a Microfuge. The cell pellet was combined with the other cells in the PBS aliquot; the sonication, chilling, and vortexing procedure was repeated for two additional cycles. Plate counts were performed as described above.

Electron microscopy. Separate tube biofilm experiments were inoculated with PAO1 *lasB*::*gfp* or MJK3. After 3 days of growth at 30°C, the silicone tubing was sliced open, and scanning electron microscopy (SEM) was performed as previously described (32). Planktonic cultures of PAO1 *lasB*::*gfp* and MJK3 were grown with shaking at 37°C, and aliquots were dropped onto Formvar-coated copper slot grids and allowed to air dry. These preparations were negatively stained with 2% uranyl acetate and examined with a JEOL 100CX transmission electron microscope at 80 kV and magnification of ×48,000.

Biofilm daughter cell analysis. The movement and behavior of individual cells of PAO1 and MJK8 were examined in young biofilms (<12 h after inoculation) in flow cells. The flow cell setup was the same as described above. Phase-contrast micrographs were taken every 2 minutes using the time-lapse feature of the Zeiss Axiophot microscope (Carl Zeiss, Inc., Jena, Germany) and camera (Axiocam; Carl Zeiss, Inc., Jena, Germany). Bacterial movements were visually tracked in the images, and each cell was classified as a squatter, flyer, or rambler according to the method of Singh et al. (33). From one cell division to the next, squatters remained within a 15-μm-diameter circle centered at the point of parental cell division, ramblers moved outside this 15-μm circle, and flyers were simply removed from the surface by the medium flow. Seventy cells of each strain were tracked and classified in this manner.

Transcriptional profiling and analysis. Cultures were grown in 250-ml baffled Erlenmeyer flasks containing 50 ml LB and a stir bar. Each strain (PAO1, MJK3, MJK8, MJK22, and MJK123) was grown in triplicate. The cultures were incubated at 37°C and shaken at 100 rpm. When the OD_{600} reached 0.25, the cultures were placed on ice. RNA was extracted from two aliquots with an RNeasy kit (QIAGEN, Inc., Valencia, CA) according to the manufacturer's instructions. RNA from all replicate samples was combined at this point. Contaminating DNA was removed with an on-column RNase-free DNase I treatment (QIAGEN, Inc.,

Valencia, CA); remaining DNA was removed by an off-column DNase I treatment (0.1 U/μg RNA) at 37°C for 30 min. DNase I was removed by repurifying the RNA with an RNeasy column. The quality of the RNA was verified by gel electrophoresis, and the quantity of the RNA was assessed spectrophotometrically.

cDNA was prepared from RNA according to the procedure of Schuster et al. (31). Each cDNA reaction mixture contained 12 μg test RNA, 1 to 10 pM control RNA (*Saccharomyces cerevisiae*, *Bacillus subtilis*, and *Arabidopsis* RNA), 12.5 ng/μl semirandom decamer (75% G+C content), and 1,500 U of Superscript II (Invitrogen, Carlsbad, CA). The reactions were incubated at 25°C for 10 min, 37°C for 60 min, and 42°C for 60 min, followed by enzyme inactivation at 70°C for 10 min. Following cDNA synthesis, RNA was removed by alkaline hydrolysis. cDNA was purified with a QIAquick kit (QIAGEN, Inc., Valencia, CA) and fragmented with 0.05 U DNase I/μg cDNA. The fragments were labeled at the 3′ end with biotin-ddUTP, and these labeled fragments were then hybridized to the Affymetrix GeneChip *P. aeruginosa* genome array.

One array was run for each of the ST strains (MJK3, MJK8, MJK22, and MJK123), and two arrays were run for PAO1 (control strain). Transcript levels of the ST strains were compared to the transcript levels of PAO1 using the Affymetrix Microarray software suite (version 5.0). The software employs a statistical algorithm that determines if a transcript level is significantly increased, significantly decreased, or shows no change in comparison to the transcript level of the control. The 4 ST arrays were individually compared to the 2 WT arrays for a total of 8 comparisons.

RESULTS

Biofilm growth of *P. aeruginosa* produces sticky colony morphology variants. *P. aeruginosa* biomass harvested from a tube biofilm reactor produced two prevalent colony morphologies: the wild-type PAO1 colony morphology (Fig. 1a) and the smaller, wrinkled, "sticky" colony morphology (Fig. 1b). ST was thus named due to its strong aggregative phenotype in liquid culture (compare Fig. 1c and d) and its hyperadherence to abiotic surfaces. On solid growth medium, the ST variant formed colonies that were smaller and had a rough, wrinkled, and dry surface appearance compared to the smooth, larger WT colonies. This rough, wrinkled appearance was also evident upon comparing SEM analysis of WT and ST biofilms grown in silicone tubing (compare Fig. 1e and f). Furthermore, when plated onto solid medium containing Congo red, the ST variant displayed a deep red color, while WT was light brown (data not shown).

Despite the aggregative phenotype of ST, the doubling times of WT and ST in liquid culture were comparable (33 and 25 min, respectively), as calculated by measuring OD_{600} or total protein in the culture over time (data not shown). As shown in Fig. 2, when tube biofilm reactors were inoculated with PAO1, ST was commonly isolated from the reactor. Ultimately, ST accounted for less than 20% of the total biofilm population and first appeared approximately 40 h after inoculation of the system. Figure 2 shows that ST isolates were absent in some of the harvested biofilms or were present at levels below the detection limit.

We verified that the ST phenotype was not a contaminant using T-RFLP of an amplified segment of the 16S rDNA (data not shown). Furthermore, our data suggest that it is a stable genotypic variant of WT, since no revertants were found after numerous subculturings in liquid medium and after biofilm growth (data not shown).

Survey of ST and WT phenotypes. Several reports in the literature describe *P. aeruginosa* colony morphology variants that are similar in appearance to ST. Many phenotypic traits associated with these variants are similar across the studies, but some discrepancies exist. Therefore, we surveyed a number of phenotypes that have been associated with these variants.

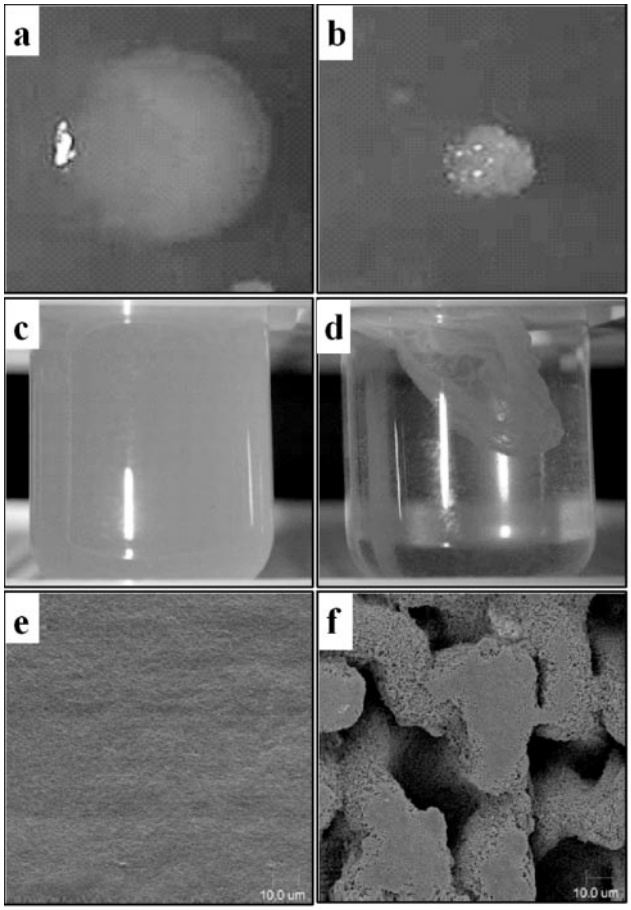

FIG. 1. Appearance of WT (PAO1 *lasB*::*gfp*) and ST (MJK3) colony morphology variants on solid medium and in liquid culture. When grown on solid medium, the wild-type strain formed large flat colonies (a), whereas ST formed small, wrinkled, sticky colonies (b). In shaken liquid culture, WT yielded a homogeneous culture (c), but ST tended to grow as a clump (d). As shown by SEM, a WT tube biofilm was flat (e), and an ST tube biofilm had an irregular, wrinkled surface (f). Magnification, ×1,000.

The cohesiveness of ST cells suggests increased hydrophobicity, so relative hydrophobicity of the ST isolates was evaluated using the MATH test. Eleven independent ST isolates were tested, but for clarity, only the results from 3 ST isolates

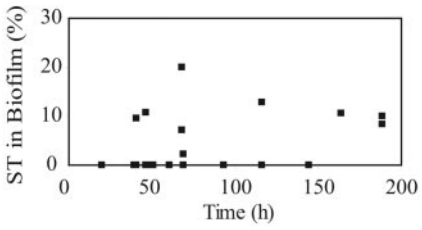

FIG. 2. Frequency of ST isolates in a tube biofilm reactor. Each datum point is the average of the results from three replicate viable plate counts. ST colonies were typically found in the biofilm after 40 h of culturing.

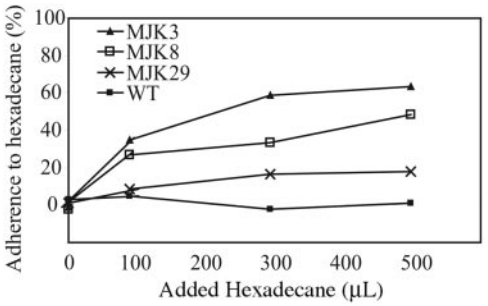

FIG. 3. Adherence to hexadecane as a measure of relative hydrophobicity. Each datum point is based on the results from three replicate OD measurements. PAO1 and three independent ST isolates were assayed for relative hydrophobicity using the MATH test. ST isolates typically had increased hydrophobicities compared to the WT, but the hydrophobicities of the ST isolates were variable.

are shown in Fig. 3. In general, the ST isolates were more hydrophobic than those of the WT. However, as evidenced by the results from MJK3, MJK8, and MJK29, the relative hydrophobicities of the ST isolates were variable.

Previous reports in the literature have also linked similar colony morphology variants to changes in antibiotic susceptibility, so we tested planktonic and biofilm cells of WT and ST for their relative susceptibilities to tobramycin and chlorine. For a valid comparison of antibiotic tolerance between WT and ST, the same number of cells must be challenged with the antibiotic for each strain. Therefore, we used specific culturing conditions in a spinning disk biofilm reactor that allowed the generation of biofilms with equal numbers of cells. An analysis of the survival rates as a function of applied biocide concentration indicated that biofilms of the ST variant were more resistant to tobramycin than were WT biofilms (Fig. 4), even though planktonic cells of WT and ST had similar resistances to tobramycin (data not shown). As expected, WT and ST biofilms were more resistant to tobramycin than were their planktonic counterparts (data not shown). On the other hand, when challenged with chlorine, ST and WT biofilms showed the same degree of resistance, as did planktonic cultures of ST and WT (data not shown). Thus, increased antimicrobial resistance does not appear to be a general trait of the ST colony morphology.

The twitching and swimming motility phenotypes of the variants were examined. All ST isolates showed impaired swimming (Fig. 5a) and twitching (Fig. 5b) motilities compared to

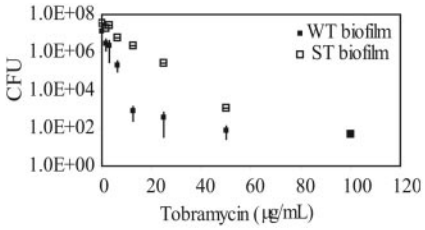

FIG. 4. Tobramycin resistance of WT (PAO1) and an ST variant (MJK8) biofilm cells. Each datum point is the average of the results from four replicate experiments, and the error bars represent one standard deviation. ST biofilms showed greater resistance to tobramycin than did WT biofilms.

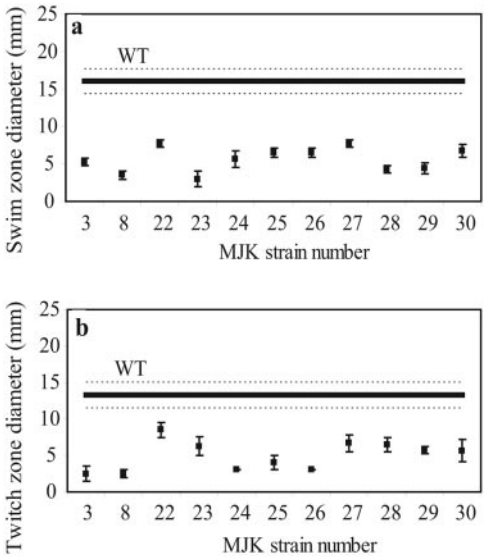

FIG. 5. Swimming (a) and twitching (b) motilities of the WT (PAO1) versus independent isolates of ST variants. Each datum point is the average of the results from four replicate measurements; the dashed lines and error bars represent one standard deviation. The swimming and twitching motilities were variable among the ST isolates but were always less than those of PAO1.

the WT. Although these independently generated ST isolates were indistinguishable from one another in terms of colony morphology, Fig. 5a and b demonstrate that they were heterogeneous in terms of their relative motilities. Furthermore, phenotypic heterogeneity was present not only in ST isolates but in WT colony morphology isolates as well. We randomly chose 20 WT isolates from a 6-day-old WT tube biofilm and tested their swimming motilities. The 20 WT biofilm isolates showed great variation in swimming motility (19% to 115% of the swimming motility of the WT parent strain) (data not shown). While a few isolates had swimming motilities close to that of the WT parent strain, most had swimming motilities that were intermediate between WT and ST. The heterogeneity in swimming motility was stable even after several subculturings, indicating a heritable genetic change. This variability was not observed in a control planktonic culture.

The ST variant has a hyper-biofilm-forming phenotype. ST and WT biofilm formation was examined further using a flow cell biofilm reactor system. Based on visual inspection, ST formed biofilms with more biomass and distinct three-dimensional architecture than WT biofilms (Fig. 6a). Similarly, after extended growth in a tube biofilm (~200 h), an ST biofilm had 2 orders of magnitude more biomass per unit area than the comparable WT biofilm (10^{10} CFU/mm^2 versus 10^8 CFU/mm^2). In a microtiter plate adhesion assay, an ST variant (MJK8) showed four times greater crystal violet stainable biofilm biomass than did PAO1, verifying that ST has a hyper-biofilm-forming phenotype (Fig. 7a).

Because surface-associated motility has been implicated in *P. aeruginosa* biofilm development and the ST variants exhibit reduced surface motility, we examined the potential relationship between surface-associated motility and the observed structural differences in WT and ST biofilm architecture. The

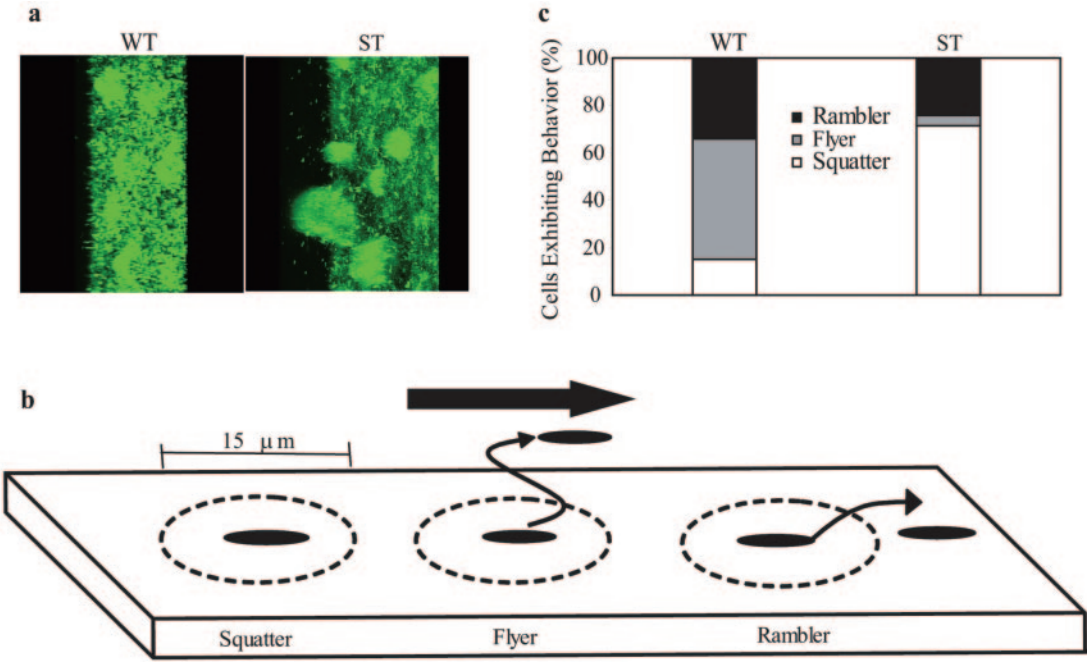

FIG. 6. Correlation between surface-associated motility and biofilm architecture. (a) Representative LS images of flow cell biofilms of WT (PAO1) and ST (MJK8). These strains were constitutively producing green fluorescent protein (GFP) from the GFP expression vector pMRP9. (b) Squatter-flyer-rambler definition. The large arrow at the top indicates the direction of liquid flow. (c) Biofilm daughter cell analysis of 70 cells of each strain. Most progeny of a developing PAO1 biofilm were released into the bulk liquid or moved on the surface, while most ST daughter cells stayed associated with the biofilm and remained in place.

movements of 70 randomly selected, newly adherent cells of WT and of ST were tracked on a surface using time-lapse microscopy from one cell division to the next. We categorized the surface-associated behavior of each cell according to the method of Singh et al. (33). Three categories of behavior were defined: daughter cells that were released into the bulk liquid were termed flyers, daughter cells that remained adherent to the surface and showed limited movement were called squatters, and daughter cells that moved extensively on the surface were called ramblers (Fig. 6b). Our analysis (Fig. 6c) demonstrated that WT cells were very mobile, and many progeny were released into the bulk liquid (34% ramblers and 51% flyers), while the ST cells tended to remain close to the point of initial attachment (71% squatters) and daughter cells remained associated with the biofilm.

a

Strain	OD_{595nm}	Standard deviation
PAO1	0.34	0.03
PAO1-*psl*	0.27	0.02
MJK8	1.31	0.18
MJK8-*psl*	0.36	0.05

b

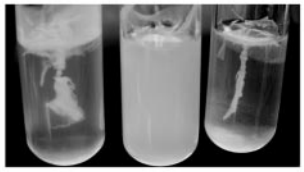

FIG. 7. Microtiter plate adhesion assay and liquid culture phenotype showing the effect of the *psl* locus on biofilm formation. (a) ST (MJK8) showed greater biofilm adhesion than did WT (PAO1) in a microtiter plate assay; however, a *psl* mutant in the ST background (MJK8-*psl*) showed biofilm adhesion similar to that of WT. Each datum point is the average of the results from duplicate experiments. (b) MJK8-*psl* showed homogeneous growth in shaken liquid culture, as opposed to the aggregation of MJK8. When MJK8-*psl* was complemented with pMO011305, aggregation was restored in liquid culture.

Transcriptional profiling of ST variants. Using Affymetrix DNA microarrays, we compared transcriptional profiles of WT and ST liquid cultures. Due to the variability seen in phenotypes associated with different ST isolates, transcriptional profiles of four independently obtained ST isolates (MJK3, MJK8, MJK22, and MJK123) were compared to the WT parent to identify differentially regulated genes common to the ST phenotype, not particular to any one variant. Cells were grown to mid-log phase in planktonic culture, and their mRNA was harvested and processed for DNA microarray analyses.

Figure 8 and Table 2 highlight some of the genes that were differentially expressed between the WT and the four ST isolates in liquid culture. A cluster of putative bacteriophage genes (PA0717 to PA0728) was prominently down-regulated; furthermore, all of the ST isolates showed down-regulation of genes related to flagellum functions. Most of the isolates showed increased expression of genes related to type IV pili biosynthesis. Other induced genes included the *psl* locus (PA2231 to PA2245) and the *pel* locus (PA3058 to PA3064),

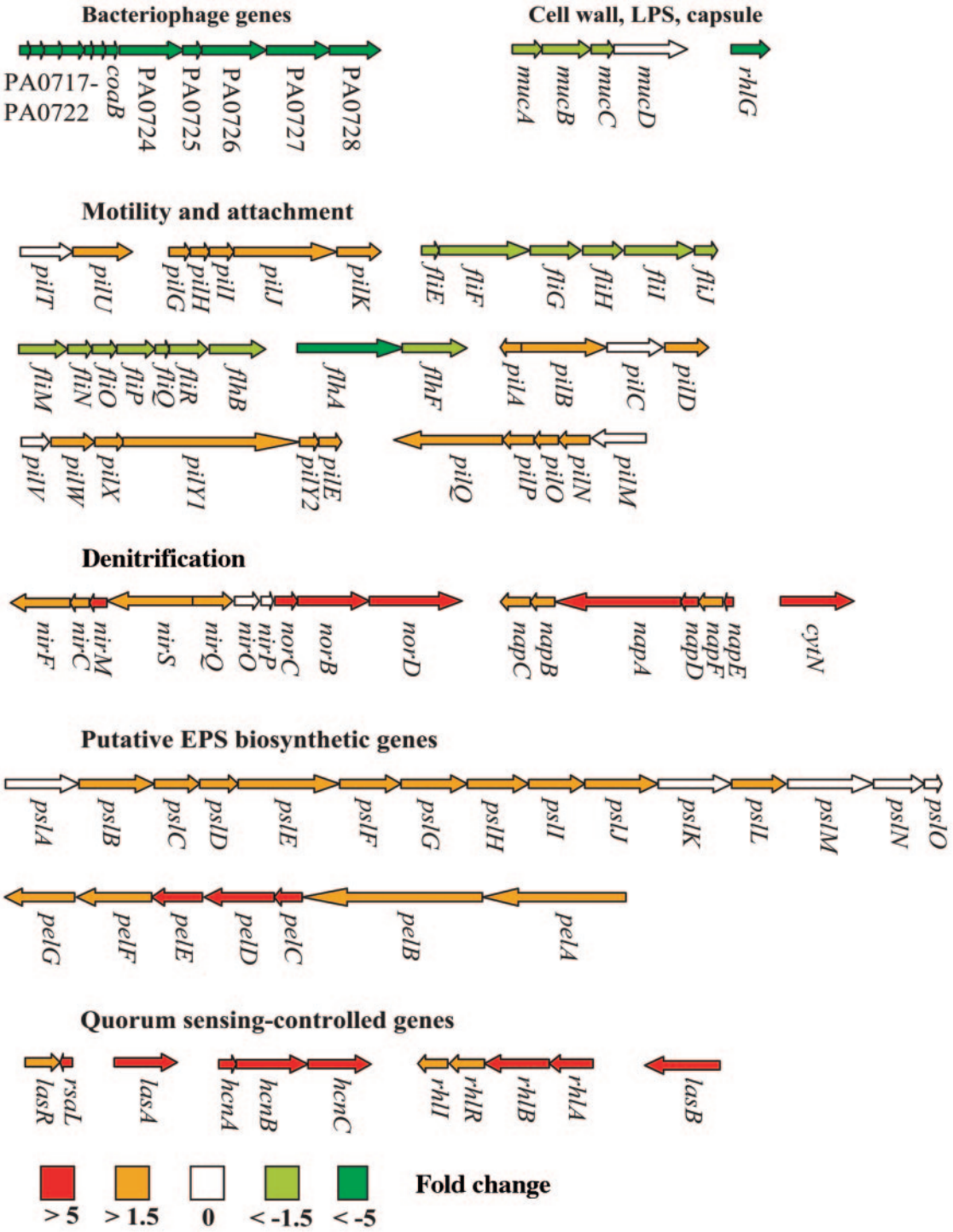

FIG. 8. Differential gene expression in selected genes in ST (MJK3, MJK8, MJK22, and MJK123) compared to WT (PAO1) and organization of differentially regulated genes. Putative operons are indicated by connected arrows. The direction of the arrow shows the gene direction, and the color of the arrow shows the geometric mean of up- or down-regulation in ST compared to that in WT. LPS, lipopolysaccharide.

which have been implicated in exopolysaccharide production and biofilm formation.

A distinct issue in interpreting the array data is the strong autoaggregative phenotype of the ST variants in liquid culture. Although great care was taken to minimize aggregation in the cultures, some was still evident. The two most pronounced effects probably due to aggregation were early induction of quorum-sensing-regulated genes and induction of some of the genes involved in denitrification (Fig. 8; Table 2). Using a *lasB*::*gfp* transcriptional fusion (*lasB* encodes the quorum-sens-

TABLE 2. Differential gene expression in selected genes in ST (MJK3, MJK8, MJK22, and MJK123) compared to WT (PAO1)

Gene type and no.[a]	Description[b]	Fold geometric mean change (×/÷geometric SD)[c]
Bacteriophage		
PA0717	Hypothetical protein of bacteriophage Pf1	−70.4 (1.3)
PA0718	Hypothetical protein of bacteriophage Pf1	−65.7 (1.4)
PA0719	Hypothetical protein of bacteriophage Pf1	−102.2 (1.4)
PA0720	Helix-destabilizing protein of bacteriophage Pf1	−48.1 (1.4)
PA0721	Hypothetical protein of bacteriophage Pf1	−220.9 (1.9)
PA0722	Hypothetical protein of bacteriophage Pf1	−65.7 (1.3)
PA0723	*coaB*, coat protein B of bacteriophage Pf1	−40.1 (1.2)
PA0724	Probable coat protein A of bacteriophage Pf1	−176.4 (1.5)
PA0725	Hypothetical protein of bacteriophage Pf1	−104.0 (1.6)
PA0726	Hypothetical protein of bacteriophage Pf1	−58.7 (1.1)
PA0727	Hypothetical protein of bacteriophage Pf1	−49.4 (1.3)
PA0728	Probable bacteriophage integrase	−122.6 (1.9)
Cell wall, LPS, capsule		
PA0763	*mucA*, anti-sigma factor MucA	−1.7 (1.1)
PA0764	*mucB*, negative regulator for alginate biosynthesis MucB	−3.1 (1.2)
PA0765	*mucC*, positive regulator for alginate biosynthesis MucC	−4.1 (1.3)
PA0766[d]	*mucD*, serine protease MucD precursor	−1.3 (1.2)
PA3387	*rhlG*, beta-ketoacyl reductase	−12.9 (1.6)
Flagellar motility		
PA1100	*fliE*, flagellar hook-basal body complex protein FliE	−4.4 (1.3)
PA1101	*fliF*, flagellar M-ring outer membrane protein precursor	−3.0 (1.3)
PA1102	*fliG*, flagellar motor switch protein FliG	−3.0 (1.4)
PA1103	*fliH*, probable flagellar assembly protein	−2.2 (1.2)
PA1104	*fliI*, flagellum-specific ATP synthase FliI	−2.3 (1.1)
PA1105	*fliJ*, flagellar protein FliJ	−4.8 (1.4)
PA1443	*fliM*, flagellar motor switch protein FliM	−2.1 (1.2)
PA1444	*fliN*, flagellar motor switch protein FliN	−1.9 (1.2)
PA1445	*fliO*, flagellar protein FliO	−2.7 (1.3)
PA1446	*fliP*, flagellar biosynthesis protein FliP	−2.0 (1.2)
PA1447	*fliQ*, flagellar biosynthesis protein FliQ	−1.8 (1.2)
PA1448	*fliR*, flagellar biosynthesis protein FliR	−2.0 (1.1)
PA1449	*flhB*, flagellar biosynthesis protein FlhB	−1.9 (1.3)
PA1452	*flhA*, flagellar biosynthesis protein FlhA	−6.3 (1.5)
PA1453	*flhF*, flagellar biosynthesis protein FlhF	−2.7 (1.3)
Denitrification		
PA0516	*nirF*, heme d1 biosynthesis protein NirF	3.3 (1.4)
PA0517	*nirC*, probable cytochrome *c*-type precursor	3.2 (1.4)
PA0518	*nirM*, cytochrome c-551 precursor	5.1 (1.4)
PA0519	*nirS*, nitrate reductase precursor	4.0 (1.3)
PA0520	*nirQ*, regulatory protein NirQ	2.4 (1.3)
PA0521	*nirO*, probable cytochrome *c* oxidase subunit	None
PA0522	*nirP*, hypothetical protein	None
PA0523	*norC*, nitric oxide reductase subunit C	8.4 (1.4)
PA0524	*norB*, nitric oxide reductase subunit B	6.9 (1.4)
PA0525	*norD*, probable denitrification protein NorD	16.0 (1.7)
PA1172[d]	*napC*, cytochrome *c*-type protein NapC	4.7 (1.6)
PA1173[d]	*napB*, cytochrome *c*-type protein NapB precursor	4.7 (1.7)
PA1174	*napA*, periplasmic nitrate reductase protein NapA	7.1 (1.4)
PA1175[d]	*napD*, periplasmic nitrate reductase protein NapD	5.2 (1.6)
PA1176[d]	*napF*, ferrodoxin protein NapF	4.8 (1.6)
PA1177[d]	*napE*, periplasmic nitrate reductase protein NapE	8.1 (2.1)
PA4133	*cytN*, cytochrome *c* oxidase subunit (cbb3 type)	18.1 (3.0)
Putative EPS biosynthesis		
PA2231	*pslA*, probable glycosyl transferase	None
PA2232	*pslB*, probable phosphomannose isomerase/GDP-mannose pyrophosphorylase	2.6 (1.3)
PA2233[d]	*pslC*, probable glycosyl transferase	2.4 (1.4)
PA2234	*pslD*, probable exopolysaccharide transporter	2.7 (1.3)
PA2235[d]	*pslE*, hypothetical protein	2.1 (1.2)
PA2236[d]	*pslF*, hypothetical protein	2.2 (1.2)
PA2237[d]	*pslG*, probable glycosyl hydrolase	2.3 (1.4)
PA2238[d]	*pslH*, hypothetical protein	2.4 (1.2)
PA2239[d]	*pslI*, probable transferase	2.0 (1.2)
PA2240[d]	*pslJ*, hypothetical protein	2.1 (1.2)
PA2241	*pslK*, hypothetical protein	None
PA2242[d]	*pslL*, hypothetical protein	1.7 (1.1)

Continued on following page

TABLE 2—*Continued*

Gene type and no.[a]	Description[b]	Fold geometric mean change (×/÷geometric SD)[c]
PA2243	*pslM*, hypothetical protein	None/decrease
PA2244	*pslN*, hypothetical protein	None
PA2245	*pslO*, hypothetical protein	None/decrease
PA3058[d]	*pelG*, hypothetical protein	2.9 (1.5)
PA3059	*pelF*, hypothetical protein	4.5 (1.4)
PA3060	*pelE*, hypothetical protein	9.1 (2.1)
PA3061	*pelD*, hypothetical protein	6.4 (1.2)
PA3062	*pelC*, hypothetical protein	9.4 (1.2)
PA3063[d]	*pelB*, hypothetical protein	3.6 (1.3)
PA3064[d]	*pelA*, hypothetical protein	4.9 (2.2)
Type IV pilus function		
PA0395	*pilT*, twitching motility protein PilT	None
PA0396[d]	*pilU*, twitching motility protein PilU	2.1 (1.2)
PA0408[d]	*pilG*, twitching motility protein PilG	1.5 (1.1)
PA0409[d]	*pilH*, twitching motility protein PilH	1.8 (1.2)
PA0410[d]	*pilI*, twitching motility protein PilI	1.9 (1.1)
PA0411[d]	*pilJ*, twitching motility protein PilJ	2.3 (1.3)
PA0412[d]	*pilK*, methyltransferase PilK	2.0 (1.1)
PA4525	*pilA*, type IV fimbrial precursor PilA	2.7 (1.3)
PA4526[d]	*pilB*, type IV fimbrial biogenesis protein PilB	2.0 (1.3)
PA4527	*pilC*, still frameshift type IV fimbrial biogenesis protein PilC	None
PA4528[d]	*pilD*, type IV prepilin peptidase PilD	1.6 (1.0)
PA4551	*pilV*, type IV fimbrial biogenesis protein PilV	None
PA4552[d]	*pilW*, type IV fimbrial biogenesis protein PilW	1.9 (1.2)
PA4553[d]	*pilX*, type IV fimbrial biogenesis protein PilX	2.3 (1.2)
PA4554[d]	*pilY1*, type IV fimbrial biogenesis protein PilY1	1.9 (1.1)
PA4555	*pilY2*, type IV fimbrial biogenesis protein PilY2	2.5 (1.2)
PA4556	*pilE*, type IV fimbrial biogenesis protein PilE	2.3 (1.5)
PA5040	*pilQ*, type IV fimbrial biogenesis protein outer membrane protein PilQ precursor	2.1 (1.2)
PA5041	*pilP*, type IV fimbrial biogenesis protein PilP	1.8 (1.1)
PA5042	*pilO*, type IV fimbrial biogenesis protein PilO	1.7 (1.1)
PA5043[d]	*pilN*, type IV fimbrial biogenesis protein PilN	1.7 (1.0)
PA5044	*pilM*, type IV fimbrial biogenesis protein PilM	None
Quorum sensing controlled		
PA1430[d]	*lasR*, transcriptional regulator LasR	2.4 (1.3)
PA1431	*rsaL*, regulatory protein RsaL	9.8 (1.5)
PA1871[d]	*lasA*, protease precursor LasA	13.9 (2.3)
PA2193	*hcnA*, hydrogen cyanide synthase HcnA	13.7 (2.4)
PA2194	*hcnB*, hydrogen cyanide synthase HcnB	9.0 (2.1)
PA2195	*hcnC*, hydrogen cyanide synthase HcnC	19.5 (2.4)
PA3476	*rhlI*, autoinducer synthesis protein RhlI	3.6 (1.5)
PA3477[d]	*rhlR*, transcriptional regulator RhlR	3.4 (1.2)
PA3478[d]	*rhlB*, rhamnosyltransferase chain B	5.3 (1.5)
PA3479[d]	*rhlA*, rhamnosyltransferase chain A	7.6 (1.5)
PA3724[d]	*lasB*, elastase LasB	76.1 (1.8)

[a] Gene numbers are from the *Pseudomonas* genome project (www.pseudomonas.com).
[b] Protein descriptions are from the *Pseudomonas* genome project (18).
[c] Negative change means that the genes were down-regulated in ST compared to WT. Positive change means that the genes were up-regulated in ST compared to WT.
[d] Fewer than 8 of 8 comparisons were up-regulated or down-regulated.

ing-regulated protease elastase), we verified that quorum-sensing-regulated genes were induced early in an ST culture where a small amount of cellular aggregation was evident compared to a WT culture (data not shown). We believe that early induction is due to aggregation, although we cannot rule out that expression of the quorum-sensing regulatory machinery is elevated in the ST variant background.

Overexpression of the *psl* locus contributes to hyperadherence in the ST background. Array data suggested that the *psl* locus was up-regulated in the ST background (Fig. 8; Table 2). Previous reports indicated that this locus plays a role in the adherence of PAO1 to surfaces (10, 18, 21); therefore, we examined the possibility that the *psl* locus may contribute to some of the characteristic phenotypes of the ST variants. Genes PA2232 to PA2235 of the *psl* locus in ST isolate MJK8 were targeted for allelic replacement, and the mutation was confirmed by PCR. The *psl* mutant (MJK8-*psl*) had no growth defect (data not shown). MJK8-*psl* looked somewhat similar to its ST parent strain on solid medium because it retained the small, wrinkled colony morphology; however, mutant colonies

TABLE 3. Biofilm adhesion and twitching motility of ST CF isolates

Strain	Biofilm adhesion assay (OD_{595} [±SD])	Twitching motility (diam [mm] [±SD])
009 37s	0.76 (0.14)	3.5 (0.7)
009 38s	0.88 (0.01)	3.0 (1.4)
009 39s	1.04 (0.18)	0.8 (1.7)
CF127	2.55 (0.21)	10.3 (1.0)
PAO1	0.56 (0.15)	12.5 (1.0)

were shiny and did not have the dry appearance of the ST parent (data not shown). Interestingly, MJK8-*psl* lost the hyperadherence phenotype (Fig. 7a) and failed to autoaggregate in liquid culture (Fig. 7b). Complementation of MJK8-*psl* with the cosmid pMO011305, which contains most of the *psl* locus (18), restored autoaggregation and hyperadherence (Fig. 7b).

We therefore decided to further investigate the possibility that differential exopolysaccharide production directed by the *psl* and *pel* loci contributed to the ST phenotype. Friedman and Kolter (10, 11) found that the *psl* and *pel* loci are associated with the production of biofilm matrices enriched in mannose and glucose, respectively, for a clinical strain that had a colony morphology phenotype similar to that of our ST isolates. Consistent with these observations, mannose was slightly enriched in the EPS from an ST isolate (MJK8) compared to the EPS in WT PAO1 (18.9% of ST EPS and 13.9% of WT EPS), while glucose increased just slightly in the ST isolate (42.7% of ST EPS and 41.0% of WT EPS).

Clinical ST isolates show phenotypes similar to those of the laboratory biofilm-derived ST isolates. Four clinical isolates, derived from CF patients, exhibited the same general appearance as the laboratory-derived ST isolates on solid growth medium, forming small, wrinkled colonies. Furthermore, the clinical strains had doubling times similar to that of PAO1 (data not shown). Other phenotypes were consistent with our laboratory-derived ST isolates, including aggregation in liquid culture (data not shown), hyperadherence in a microtiter plate adhesion assay (Table 3), and reduced motility (Table 3).

Is the sticky variant adapted to a particular biofilm niche? One interpretation of our initial observation is that environmental conditions within a developing biofilm select for the ST phenotype. In an attempt to identify conditions that may select for the ST variant in liquid culture, we exposed PAO1 planktonic cells to a wide variety of culturing conditions, including variable pH, oxidative stress, osmotic stress, variable nutrient conditions/starvation, and anaerobiosis. We also subjected PAO1 to spent culture fluid isolated from stationary-phase cultures. In shaken liquid culture, none of these conditions generated ST variants, even after a prolonged exposure time (15 days) (data not shown). At the end of this period, these same batch cultures were stagnated for 12 days, after which time ST variants were observed (data not shown). The ST variants comprised 16 to 94% of the total CFU, with the greatest numbers of ST variants generally occurring in the defined media (Jensen's, M9, and EPRI).

In laboratory-grown biofilms, we noted that ST isolates never exceeded ~20% of the total cells in a biofilm community (Fig. 2). This is contrary to what one might predict, since ST cells are hyperadherent and daughter cells remain associated with the biofilm, while WT daughter cells tend to be lost to the bulk liquid (Fig. 6c). One reason to explain the inability of the ST variants to predominate in a biofilm is that they are adapted to a particular niche or region of a biofilm community. We explored this idea by analyzing biofilm communities coinoculated with ST and WT cells. We coinoculated tube biofilm reactors with various ratios of WT to ST, and the biofilm population went from approximately 1×10^6 CFU/mm^2 at early time points (20 h) to approximately 1×10^8 CFU/mm^2 at late time points (140 h). When the reactors were inoculated with WT-to-ST ratios of 93:7, 71:29, and 24:76, the percentage of ST in the biofilm always reached a steady-state value of 28 to 43% after 6 days (Fig. 9a).

To examine the spatial distribution of WT and ST cells in a coculture biofilm, a flow cell biofilm reactor was coinoculated with a 1:1 ratio of WT to ST cells, and the locations of both types of cells were observed over time using CLSM. After 3 days of incubation, large clusters of ST cells (Fig. 9b) comprised the majority of the biofilm. Gradually, WT cells became more prevalent, and Fig. 9b (4 days) shows WT cells associated with an ST aggregate. After 8 days of incubation, WT cells appeared to outnumber the ST cells. ST cells were buried in the depths of the biofilm, covered by a carpet of WT cells (Fig.

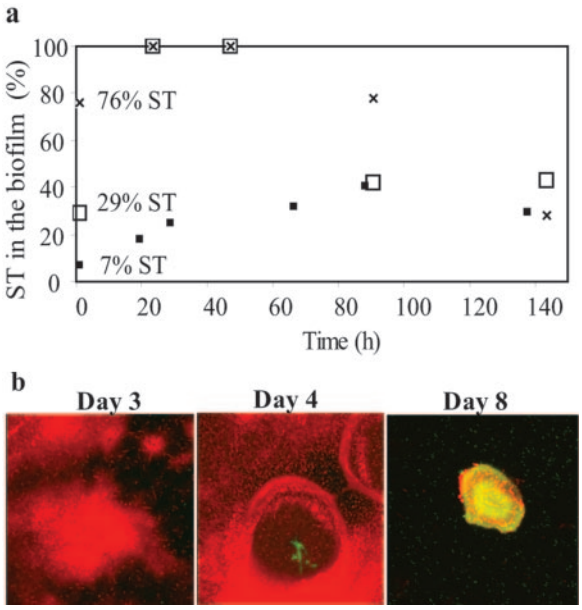

FIG. 9. WT and ST variant coculture experiments. (a) Tube biofilms were inoculated with various WT/ST ratios; WT is PAO1, and ST is MJK8. Each datum point is based on the results from three replicate viable plate counts. (b) Confocal micrographs show the progression of a coculture biofilm of WT and ST (1:1 inoculum); WT is PAO1-Tn*7-gfp*, and ST is MJK8. Biofilms were stained with Syto 62; therefore, ST cells are red and WT cells (labeled with green fluorescent protein) are green. Tube biofilm reactor experiments showed that the percentage of ST biomass in the biofilm always reached a level between 28% and 43%. This was consistent with the confocal micrographs, which showed that the ST biomass towers (red cells) predominated early on (days 3 and 4) yet ultimately gave way to WT (green cells) covering ST by day 8. The top-down view of the biofilm tower appears yellow due to the presence of both ST (red) and WT (green) fluorescent signals. Due to the depth of the biofilm, the attachment surface and its associated bacteria cannot be seen in the day 8 micrograph.

9b). Although this experiment obviously does not reflect the spatial distribution of ST cells that might spontaneously arise within a WT biofilm, the results correlate to those shown in Fig. 9a, where the initial predominance of ST cells at earlier time points is followed by biofilms containing a more even distribution of WT and ST cells.

DISCUSSION

In this study, we report that biofilm growth selects for *P. aeruginosa* colony morphology variants that have biofilm-related phenotypes. We isolated several variants that exhibit what we call the sticky, or ST, phenotype. These variants are easily identified on solid medium because of their small, wrinkled colony morphologies. All of our laboratory-derived ST isolates show hyperadherence, increased hydrophobicity, and reduced swimming and twitching motilities, although they exhibit these phenotypes to varying degrees. Transcriptional profiling of these variants suggested an up-regulation of putative EPS genes and type IV pili and down-regulation of bacteriophage genes. CF clinical isolates exhibiting the ST colony morphology were also characterized. Similar to the laboratory-derived ST isolates, the ST clinical isolates showed reduced twitching motility and hyperadherence to abiotic surfaces. Finally, when ST and WT were coinoculated in a biofilm experiment, the percentage of ST in the biofilm reached a steady-state.

As shown in Fig. 2, the isolation of ST cells from a WT biofilm is a consistent phenomenon. Furthermore, recent reports in the literature have described similar *P. aeruginosa* colony morphology variants and have linked these variants to CF and biofilm growth. For instance, *P. aeruginosa* colony morphology variants have been found in static liquid cultures and biofilms (8), in agar plate populations challenged with kanamycin (9), and in sputum and deep throat swab samples from CF patients (13, 14). Despite similar colony morphologies, phenotypic differences exist among the variants reported in the different studies. For example, our study is consistent with those of Déziel et al. (8) and D'Argenio et al. (6), who described variants with reduced twitching motility, but Häußler et al. (14) observed increased twitching motility in hyperpiliated variants from clinical samples. Such differences underscore an important point: although variants can appear quite similar on solid medium, other phenotypic characteristics may vary.

Our data suggest that phenotypic radiation in biofilms is widespread, encompassing more than colony morphology. This was highlighted by the fact that the ST variants, although indistinguishable from one another on the basis of colony morphology, differed in other phenotypic assays. We also observed significant phenotypic variation in wild-type colony morphology isolates from a 6-day-old biofilm; randomly selected isolates displayed a wide range of swimming motilities relative to that of the wild-type parent strain. Thus, while many researchers try to answer the questions related to colony morphology variation, the extent and complexity of phenotypic radiation in biofilms remain to be explored.

Transcriptional profiling highlighted several interesting genes that were differentially expressed in the ST isolates compared to the WT strain. Two up-regulated loci of interest are the *pel* (PA3058 to PA3064) and *psl* (PA2231 to PA2245) gene clusters (Fig. 8; Table 2), which have been suggested to be involved in exopolysaccharide production (glucose-rich and mannose-rich exopolysaccharides, respectively) (10, 11). While a mutation in the *psl* locus resulted in the loss of autoaggregation and hyperadherence (Fig. 7a and b), the mutated ST isolate maintained a small-colony diameter on solid growth medium, suggesting that colony morphology and hyperadherence/autoaggregation phenotypes may not be directly linked. Mutations in the *psl* locus in PAO1 have been previously shown to impair adherence to abiotic surfaces (18). Therefore, the putative EPS produced by the *psl* locus may serve as a "rheostat" for adherence. Type IV pili biogenesis genes also were up-regulated in the ST isolates (Fig. 8; Table 2), which corresponds well with transmission electron micrographs that showed hyperpiliated ST cells (data not shown). Although our ST isolates were hyperpiliated, they demonstrated a defect in twitching motility, similar to the observations of Déziel et al. (8). A locus associated with bacteriophage production (PA0717 to PA0728) was the most highly down-regulated locus in the ST isolates (Fig. 8; Table 2), but the reason for this is unclear. Whiteley et al. (39) demonstrated that this locus was among the most highly up-regulated in wild-type PAO1 biofilms. Interestingly, a recent report by Webb et al. (38) suggested that production of Pf1 filamentous phage may be instrumental in the hyperadherence and autoaggregation of colony morphology variants similar to our ST variants. Our data suggest against such a role for the bacteriophage, with the putative *psl*-encoded polysaccharide being important for autoaggregation and hyperadherence.

The linkage of surface appendages and EPS up-regulation to colony morphology phenotypes is not a new concept. Other species use similar strategies to produce colony morphology variants. *Escherichia coli* and *Salmonella enterica* serovar Typhimurium produce a colony morphology variant called the *rdar* (*r*ed, *d*ry, *a*nd *r*ough) phenotype (27, 28). This variant forms wrinkled colonies that bind the dye Congo red and is characterized by overproduction of thin aggregative fimbriae called curli and production of the exopolysaccharide cellulose. *Vibrio cholerae* produces a small, rugose colony morphology that is characterized by overproduction of the exopolysaccharide EPS^{ETr} (42). Finally, *Pseudomonas fluorescens* produces a wrinkled colony variant called the "wrinkly spreader" that results from overproduction of acetylated cellulose (34). It is unclear if similar environmental stimuli select for colony morphology variation in all of these species.

D'Argenio et al. (6) found that a mutation in *wspF* (PA3703) produced the wrinkled phenotype in *P. aeruginosa*. Comparison to homologous proteins in *E. coli* led them to theorize that the *wspF* mutation resulted in constitutive activation of WspR (encoded by PA3702). Our microarray analysis showed no change in expression of *wspR* in the ST isolates compared to the WT strain (data not shown), although this result does not rule out a WspR-mediated mechanism involving posttranscriptionally regulated activity. Drenkard and Ausubel (9) found that overexpression of *pvrR* (phenotype variant regulator) in *P. aeruginosa* PA14 caused a decrease in the number of colony variants. Our microarray analysis did not consistently implicate *pvrR* (PA3947, the closest homolog of *pvrR* in *P. aeruginosa* PAO1) in the appearance of ST. *pvrR* expression was decreased in 50% of the pairwise comparisons for MJK3, MJK8,

and MJK123 to PAO1 (data not shown). Although the array data do not implicate either the *wsp* locus or *pvrR* in the ST phenotype, we cannot rule out their involvement.

von Götz et al. (37) performed a transcriptional analysis of an SCV isolated from a CF lung. Our data overlapped with only 6 of 66 genes chosen for discussion in that study. Both data sets showed the up-regulation of PA1708 (*popD*), which is a gene in the type III secretion system; PA3790 (*oprC*), which codes for an outer membrane protein; PA2827, which may be related to oxidative stress protection (37); and PA3049 (*rmf*), which encodes a ribosome modulation factor that is essential for cellular survival under conditions of decreased growth rate (41). Additionally, PA2477 and PA2478, which encode for probable thiol-disulfide interchange proteins, were down-regulated in both data sets.

A *P. aeruginosa retS* mutant displayed hyperadherence (12), but *retS* was neither up- nor down-regulated in our ST variants. The *retS* mutant showed up-regulation of genes for exopolysaccharide synthesis, contributing to its hyper-biofilm formation, but down-regulation of the type III secretion system, resulting in a loss of cytotoxicity. A comparison of the transcriptional analyses of our ST variants and the *retS* mutant revealed a number of important similarities. For example, *pslB-pslJ* and *pslL* (PA2232 to PA2240, PA2242) and *pelF-pelC* and *pelA* (PA3059 to PA3062, PA3064) were up-regulated in our ST variants and in the *retS* mutant. However, only a minimal overlap was noted between the two data sets for the type III secretion system genes. While 40 genes of the type III secretion system were down-regulated in the *retS* mutant, only 6 of these genes were down-regulated in the ST variants, including *pscT*, *pscS*, *pscR*, *exsB*, *exsD*, and *pscC* (PA1691 to PA1693, PA1712, PA1714, and PA1716). Interestingly, comparison of the transcriptional analyses of the ST variants and the *retS* mutant also highlighted an important difference. While the ST variants showed up-regulation of many of the *pil* genes, the *retS* mutant showed down-regulation of the same genes. These genes included *pilU*, *pilG-pilK*, *pilB*, *pilD*, *pilV-pilX*, *pilY1*, *pilY2*, *pilE*, and *pilQ-pilM* (PA0396, PA0408 to PA0412, PA4526, PA4528, PA4551 to PA4553, PA4554, PA4555, PA4556, and PA5040 to PA5044).

At least two classes of genes were probably up-regulated as a consequence of the ST isolates' autoaggregation. Denitrification metabolic genes were likely up-regulated in the ST aggregates because of the reduced oxygen tension in the interior of ST aggregates. von Götz et al. (37) performed a transcriptional analysis of a colony morphology variant, and they also found increased expression of genes related to denitrification (e.g., *modA* and *modB*, which encode molybdenum transport, were up-regulated); they concluded that their variant may be "especially adapted" to the anaerobic conditions of the CF lung. Quorum-sensing-regulated genes were also up-regulated in our ST isolates, which probably results from premature induction of quorum sensing due to the high local cell densities present in aggregates.

Why do ST variants arise in a biofilm community? One possibility is that they successfully compete in a particular biofilm niche. Rainey and Travisano (25) noted the appearance of colony morphology variants in standing liquid cultures of *P. fluorescens* but not in shaken liquid cultures. They proposed and ultimately demonstrated that these variants were adapted to specific niches in the standing liquid culture. Similarly, we did not isolate the ST variant in a shaken liquid culture inoculated with WT, but we did find the ST variant in standing liquid cultures and in biofilms. We propose that the ST variant may have a competitive advantage in a particular niche of a structured system, such as a biofilm.

Based on the ST phenotype's increased adherence in short-term adhesion assays (Fig. 7a), its tendency to stay near the point of initial attachment in a biofilm (Fig. 6c), and its ability to form large cellular aggregates (Fig. 1d), one might expect ST to predominate in a biofilm inoculated with a mixture of WT and ST cells. Our WT/ST coinoculation biofilm studies (Fig. 9a) showed that even when a biofilm is inoculated with greater numbers of ST cells than WT cells, ST does not predominate once steady state is achieved. At early time points (1 and 2 days), the biofilms inoculated with 29% ST and 76% ST consisted almost entirely of ST cells (Fig. 9a). This is consistent with the daughter cell analysis of a young biofilm (Fig. 6c), which showed that ST daughter cells tended to remain associated with the biofilm, while WT daughter cells tended to be released to the bulk liquid. The biofilms inoculated with 7% ST were not dominated by ST cells at early time points. The daughter cell analysis of a young biofilm (Fig. 6c) predicts that approximately seven times as many WT cells as ST cells will be retained in a young biofilm inoculated with a 7% ST–93% WT ratio, possibly giving the WT a better chance to establish itself early in biofilm development. (According to the data in Fig. 6c, 95.6% of the inoculated ST cells will be squatters or ramblers compared to 49.3% of the WT cells. For simplicity, consider an inoculum of 100 cells. If ST cells comprise 7% of the inoculum, then we predict that 6.67 ST cells [0.956×7 cells] remain in the biofilm. If WT cells comprise 93% of the inoculum [93 WT cells], then we predict that 45.9 WT cells [0.493×93] remain in the biofilm. Therefore, 45.9 WT cells/6.67 ST cells means that there are approximately seven times more WT cells than ST cells in the young biofilm.) At later time points, regardless of the initial WT/ST inoculation ratio, a steady state is reached. One interpretation of this data is that ST has a competitive advantage in a particular region of the biofilm. Outside that niche, the identity of which has yet to be determined, WT outcompetes ST.

Our laboratory-derived ST isolates are similar in colony morphology to the clinical variants isolated from a CF lung. Like our laboratory-derived ST isolates, the clinical ST variants showed autoaggregation in liquid culture and hyperadherence to abiotic surfaces. Unlike the clinically derived SCVs from the Häußler study (14), most of our clinical isolates (3 of the 4 tested isolates) exhibited significantly reduced twitching motility (Table 3). The isolation of similar *P. aeruginosa* colony morphology variants from CF sputum samples and laboratory biofilms provides further evidence linking CF pathogenesis and the formation of biofilm communities. Whether the appearance of these variants in CF patients correlates to the establishment of chronic infection remains to be determined. This study also suggests that biofilm growth may select for distinctive subpopulations with their own specific biofilm-related phenotypes, with colony morphology variation being just one example of a distinctive subpopulation. This is an extremely important point when considering the pathogenic potential of

a biofilm community or interpreting genomic/proteomic data that present an average of the entire community.

ACKNOWLEDGMENTS

This work was supported in part by grants from the NSF (9810378) and the NIH (GM67248-01).

We thank J. Margolis for assistance with tube biofilm experiments, G. J. Balzer for providing strains MJK8/pMRP9 and PAO1-Tn*7*-*gfp*, W. Russin for preparing the transmission electron microscopy images, M. Schuster for help with the microarray analysis, V. Chitumalla and M. Hall for screening the CF isolates, J. Burns and M. Wolfgang for providing strains, and S. Lory for providing control RNAs for the microarray analysis. We also thank D. An, G. J. Balzer, G. M. Teitzel, and P. K. Singh for fruitful discussions.

REFERENCES

1. **Amann, R. I., W. Ludwig, and K. H. Schleifer.** 1995. Phylogenetic identification and in situ detection of individual microbial cells without cultivation. Microbiol. Rev. **59:**143–169.
2. **Ausubel, F. M., R. Brent, R. E. Kingston, D. D. Moore, J. G. Seidman, J. A. Smith, and K. Struhl, ed.** 2002. Short protocols in molecular biology: a compendium of methods from current protocols in molecular biology, 5th ed. John Wiley & Sons, Inc., New York, N.Y.
3. **Bjedov, I., O. Tenaillon, B. Gérard, V. Souza, E. Denamur, M. Radman, F. Taddei, and I. Matic.** 2003. Stress-induced mutagenesis in bacteria. Science **300:**1404–1409.
4. **Boles, B. R., M. Thoendel, and P. K. Singh.** 2004. Self-generated diversity produces "insurance effects" in biofilm communities. Proc. Natl. Acad. Sci. USA **101:**16630–16635.
5. **Burns, J. L., R. L. Gibson, S. McNamara, D. Yim, J. Emerson, M. Rosenfeld, P. Hiatt, K. McCoy, R. Castile, A. L. Smith, and B. W. Ramsey.** 2001. Longitudinal assessment of *Pseudomonas aeruginosa* in young children with cystic fibrosis. J. Infect. Dis. **183:**444–452.
6. **D'Argenio, D. A., M. W. Calfee, P. B. Rainey, and E. C. Pesci.** 2002. Autolysis and autoaggregation in *Pseudomonas aeruginosa* colony morphology mutants. J. Bacteriol. **184:**6481–6489.
7. **Davies, D. G., M. R. Parsek, J. P. Pearson, B. H. Iglewski, J. W. Costerton, and E. P. Greenberg.** 1998. The involvement of cell-to-cell signals in the development of a bacterial biofilm. Science **280:**295–298.
8. **Déziel, E., Y. Comeau, and R. Villemur.** 2001. Initiation of biofilm formation by *Pseudomonas aeruginosa* 57RP correlates with emergence of hyperpiliated and highly adherent phenotypic variants deficient in swimming, swarming, and twitching motilities. J. Bacteriol. **183:**1195–1204.
9. **Drenkard, E., and F. M. Ausubel.** 2002. *Pseudomonas* biofilm formation and antibiotic resistance are linked to phenotypic variation. Nature **416:**740–743.
10. **Friedman, L., and R. Kolter.** 2004. Two genetic loci produce distinct carbohydrate-rich structural components of the *Pseudomonas aeruginosa* biofilm matrix. J. Bacteriol. **186:**4457–4465.
11. **Friedman, L., and R. Kolter.** 2004. Genes involved in matrix formation in *Pseudomonas aeruginosa* PA14 biofilms. Mol. Microbiol. **51:**675–690.
12. **Goodman, A. L., B. Kulasekara, A. Rietsch, D. Boyd, R. S. Smith, and S. Lory.** 2004. A signaling network reciprocally regulates genes associated with acute infection and chronic persistence in *Pseudomonas aeruginosa*. Dev. Cell **7:**745–754.
13. **Häußler, S., B. Tümmler, H. Weißbrodt, M. Rohde, and I. Steinmetz.** 1999. Small-colony variants of *Pseudomonas aeruginosa* in cystic fibrosis. Clin. Infect. Dis. **29:**621–625.
14. **Häußler, S., I. Ziegler, A. Löttel, F. V. Götz, M. Rohde, D. Wehmhöhner, S. Saravanamuthu, B. Tümmler, and I. Steinmetz.** 2003. Highly adherent small-colony variants of *Pseudomonas aeruginosa* in cystic fibrosis lung infection. J. Med. Microbiol. **52:**295–301.
15. **Hentzer, M., G. M. Teitzel, G. J. Balzer, A. Heydorn, S. Molin, M. Givskov, and M. R. Parsek.** 2001. Alginate overproduction affects *Pseudomonas aeruginosa* biofilm structure and function. J. Bacteriol. **183:**5395–5401.
16. **Hoang, T. T., R. R. Karkhoff-Schweizer, A. J. Kutchma, and H. P. Schweizer.** 1998. A broad-host-range Flp-FRT recombination system for site-specific excision of chromosomally-located DNA sequences: application for isolation of unmarked *Pseudomonas aeruginosa* mutants. Gene **212:**77–86.
17. **Hunt, S. M., E. M. Werner, B. Huang, M. A. Hamilton, and P. S. Stewart.** 2004. Hypothesis for the role of nutrient starvation in biofilm detachment. Appl. Environ. Microbiol. **70:**7418–7425.
18. **Jackson, K. D., M. Starkey, S. Kremer, M. R. Parsek, and D. J. Wozniak.** 2004. Identification of *psl*, a locus encoding a potential exopolysaccharide that is essential for *Pseudomonas aeruginosa* PAO1 biofilm formation. J. Bacteriol. **186:**4466–4475.
19. **Jensen, S. E., I. T. Fecycz, and J. N. Campbell.** 1980. Nutritional factors controlling exocellular protease production by *Pseudomonas aeruginosa*. J. Bacteriol. **144:**844–847.
20. **Lambertsen, L., C. Sternberg, and S. Molin.** 2004. Mini-Tn7 transposons for site-specific tagging of bacteria with fluorescent proteins. Environ. Microbiol. **6:**726–732.
21. **Matsukawa, M., and E. P. Greenberg.** 2004. Putative exopolysaccharide synthesis genes influence *Pseudomonas aeruginosa* biofilm development. J. Bacteriol. **186:**4449–4456.
22. **Muyzer, G., A. Teske, C. O. Wirsen, and H. W. Jannasch.** 1995. Phylogenetic relationships of *Thiomicrospira* species and their identification in deep-sea hydrothermal vent samples by denaturing gradient gel electrophoresis of 16S rDNA fragments. Arch. Microbiol. **164:**165–172.
23. **Oliver, A., R. Cantón, P. Campo, F. Baquero, and J. Blázquez.** 2000. High frequency of hypermutable *Pseudomonas aeruginosa* in cystic fibrosis lung infection. Science **288:**1251–1253.
24. **O'Toole, G. A., and R. Kolter.** 1998. Initiation of biofilm formation in *Pseudomonas fluorescens* WCS365 proceeds via multiple, convergent signalling pathways: a genetic analysis. Mol. Microbiol. **28:**449–461.
25. **Rainey, P. B., and M. Travisano.** 1998. Adaptive radiation in a heterogeneous environment. Nature **394:**69–72.
26. **Römling, U.** 2001. Genetic and phenotypic analysis of multicellular behavior in *Salmonella typhimurium*. Methods Enzymol. **336:**48–59.
27. **Römling, U., W. D. Sierralta, K. Eriksson, and S. Normark.** 1998. Multicellular and aggregative behaviour of *Salmonella typhimurium* strains is controlled by mutations in the *agfD* promoter. Mol. Microbiol. **28:**249–264.
28. **Römling, U., Z. Bian, M. Hammar, W. D. Sierralta, and S. Normark.** 1998. Curli fibers are highly conserved between *Salmonella typhimurium* and *Escherichia coli* with respect to operon structure and regulation. J. Bacteriol. **180:**722–731.
29. **Sauer, K., M. C. Cullen, A. H. Rickard, L. A. Zeef, D. G. Davies, and P. Gilbert.** 2004. Characterization of nutrient-induced dispersion in *Pseudomonas aeruginosa* PAO1 biofilm. J. Bacteriol. **186:**7312–7326.
30. **Schaefer, A. L., E. P. Greenberg, and M. R. Parsek.** 2001. Acylated homoserine lactone detection in *Pseudomonas aeruginosa* biofilms by radiolabel assay. Methods Enzymol. **336:**41–47.
31. **Schuster, M., C. P. Lostroh, T. Ogi, and E. P. Greenberg.** 2003. Identification, timing, and signal specificity of *Pseudomonas aeruginosa* quorum-controlled genes: a transcriptome analysis. J. Bacteriol. **185:**2066–2079.
32. **Singh, P. K., A. L. Schaefer, M. R. Parsek, T. O. Moninger, M. J. Welsh, and E. P. Greenberg.** 2000. Quorum-sensing signals indicate that cystic fibrosis lungs are infected with bacterial biofilms. Nature **407:**762–764.
33. **Singh, P. K., M. R. Parsek, E. P. Greenberg, and M. J. Welsh.** 2002. A component of innate immunity prevents bacterial biofilm development. Nature **417:**552–555.
34. **Spiers, A. J., J. Bohannon, S. M. Gehrig, and P. B. Rainey.** 2003. Biofilm formation at the air-liquid interface by the *Pseudomonas fluorescens* SBW25 wrinkly spreader requires an acetylated form of cellulose. Mol. Microbiol. **50:**15–27.
35. **Urakawa, H., T. Yoshida, M. Nishimura, and K. Ohwada.** 2000. Characterization of depth-related population variation in microbial communities of a coastal marine sediment using 16S rDNA-based approaches and quinone profiling. Environ. Microbiol. **2:**542–554.
36. **Vilain, S., P. Cosette, M. Hubert, C. Lange, G. A. Junter, and T. Jouenne.** 2004. Comparative proteomic analysis of planktonic and immobilized *Pseudomonas aeruginosa* cells: a multivariate statistical approach. Anal. Biochem. **329:**120–130.
37. **von Götz, F., S. Häussler, D. Jordan, S. S. Saravanamuthu, D. Wehmhöner, A. Strüßmann, J. Lauber, I. Attree, J. Buer, B. Tümmler, and I. Steinmetz.** 2004. Expression analysis of a highly adherent and cytotoxic small colony variant of *Pseudomonas aeruginosa* isolated from a lung of a patient with cystic fibrosis. J. Bacteriol. **186:**3837–3847.
38. **Webb, J. S., M. Lau, and S. Kjelleberg.** 2004. Bacteriophage and phenotypic variation in *Pseudomonas aeruginosa* biofilm development. J. Bacteriol. **186:**8066–8073.
39. **Whiteley, M., M. G. Bangera, R. E. Bumgarner, M. R. Parsek, G. M. Teitzel, S. Lory, and E. P. Greenberg.** 2001. Gene expression in *Pseudomonas aeruginosa* biofilms. Nature **413:**860–864.
40. **Wolfgang, M. C., B. R. Kulasekara, X. Liang, D. Boyd, K. Wu, Q. Yang, C. G. Miyada, and S. Lory.** 2003. Conservation of genome content and virulence determinants among clinical and environmental isolates of *Pseudomonas aeruginosa*. Proc. Natl. Acad. Sci. USA **100:**8484–8489.
41. **Yamagishi, M., H. Matsushima, A. Wada, M. Sakagami, N. Fujita, and A. Ishihama.** 1993. Regulation of the *Escherichia coli* rmf gene encoding the ribosome modulation factor: growth phase and growth rate-dependent control. EMBO J. **12:**625–630.
42. **Yildiz, F. H., and G. K. Schoolnik.** 1999. *Vibrio cholerae* O1 El Tor: identification of a gene cluster required for the rugose colony type, exopolysaccharide production, chlorine resistance, and biofilm formation. Proc. Natl. Acad. Sci. USA **96:**4028–4033.